

1 **Fabrication, microstructure, and properties of fired clay bricks using**
2 **construction and demolition waste sludge as the main additive**

3
4
5
6 Glaydson S. dos Reis^{1,2,7*}, Bogdan G. Cazacliu², Alexis Cothenet², Philippe Poullain³,
7 Michaela Wilhelm⁴, Carlos Hoffmann Sampaio^{1,5}, Eder Claudio Lima^{1,8}, Weslei Ambros⁶,
8 Jean-Michel Torrenti⁷

9
10
11
12 ¹*Graduate Program in Metallurgical, Mine, and Materials Engineering (PPGE3M). School of*
13 *Engineering, Federal University of Rio Grande do Sul (UFRGS), Porto Alegre, Brazil*

14 ²*IFSTTAR, MAST, GPEM, F-44344 Bouguenais, France.*

15 ³*Assitant Professor, LUNAM University, University of Nantes, GeM- UMR CNRS 6183,*
16 *Research Institute in Civil Engineering and Mechanics, France*

17 ⁴*University of Bremen, Advanced Ceramics, Am Biologischen Garten 2, IW3, 28359 Bremen,*
18 *Germany*

19 ⁵*Professor Serra Húnter Program, Department of Mine, Industrial and ICT Engineering,*
20 *Polytechnical University of Catalonia, Av. Bases de Manresa 61–63, Manresa, 08242*
21 *Barcelona, Spain*

22 ⁶*Mineral Processing Laboratory, Federal University of Rio Grande do Sul, 9500 Bento*
23 *Gonçalves Avenue, Zip Code: 91501-970 Porto Alegre, Brazil*

24 ⁷*IFSTTAR, MAST, Marne-la-Vallée, France.*

25 ⁸*Institute of Chemistry, Federal University of Rio Grande do Sul (UFRGS). Av. Bento*
26 *Gonçalves 9500, Porto Alegre, RS, Brazil.*

27
28
29 *Corresponding author: FAX + 55 (51) 3308 7070; Phone: +55 (51) 3308 7070; e-
30 mail: glaydsonambiental@gmail.com or glaydson.simoes@ufrgs.br

34 **Abstract**

35

36 Green routes to prepare or manufacture sustainable building materials have been
37 attracting much attention over the years targeting sustainability issues. In this investigation,
38 for the first time, sludge from the inert mineral part of the construction and demolition waste
39 (RA-S) is used as a primary raw material in the fabrication of fired bricks for building
40 purposes. Fired bricks fabricated with different dosages of RA-S and earth material (i.e., 0%,
41 30%, 50%, 70% and 100% by weight) were prepared and evaluated in terms of their physical
42 chemical properties. The RA-S was characterized, and the results showed that it could be
43 classified as a clayey material and richly graded silty sand according to the French
44 Standards. XRD analysis revealed that the addition of the RA sludge into raw earth material
45 provoked slightly changes in the fired bricks. The compressive strength (CS) results
46 indicated that the CS of the fired bricks increased with the addition of the RA-S from 30% to
47 70%. The highest CS was attained at the firing temperature of 800°C. The density of the fired
48 brick slightly reduced with the RA-S addition. The thermal conductivity results suggest that
49 RA-S has better insulation properties compared to earth material. The RA-S sludge can be
50 used in combination with earth material to fabricate fired bricks which can meet the
51 requirements of many Standards all over the World.

52 In the light of these results, it is possible to say that the RA-S generated from recycling inert
53 mineral part of construction and demolition waste plant is an excellent raw material to
54 prepare efficient fired bricks that can be successfully employed in the real construction
55 sector. Also, the highlighted results suggest that brickwork factories have the opportunity to
56 improve production quality while significantly reducing manufacturing time, energy
57 consumption, resource depletion and environmental impact.

58

59 **Keywords:** recycling and valorization; construction and demolition waste sludge; bricks
60 production; mechanical properties; insulation properties.

61 **1. Introduction**

62 Over the last years, especially in developing countries, serious waste management
63 problems have appeared. The reasons are derived from rapid population growth,
64 urbanization, and industrial development (Behera et al., 2017). One of the biggest challenges
65 today is to promote the proper management of the large number of solid wastes generated
66 by industrial production and consumption models. Thus, the introduction of new technologies
67 to recycle and convert waste into useful materials is crucial for environmental protection and
68 sustainable development (Behera et al., 2017; Murray, 1991). For example, the use of solid
69 waste as a target material for new construction materials, such as bricks, is a practical
70 solution to reach proper management and to reduce adverse environmental effects (Behera
71 et al., 2017).

72 Bricks have been a significant construction and building material for a long time and
73 are widely used around the world. Conventional bricks are produced from non-renewable
74 materials (Raut et al. 2011) such as clays with high firing temperature (Velasco et al., 2014)
75 or cementing materials(Poon et al., 2002; Poon et al., 2009), and thus are responsible for
76 both high energy expenditure and carbon footprint (Zhang et al., 2017).

77 Re-utilization of different residues in firedbricks production can be a successful
78 strategy, due to the waste production reduction as well as decreased clay utilization
79 (Monteiro and Vieira,2014). It is also a practical solution to reduce environmental problems
80 and costs in the building sector (Al-Fakih et al., 2019; Murmu and Patel, 2018). In the last
81 years, several types of research all over the world have been working on the production of
82 bricks from different waste materials. The following wastes are examples of exciting and
83 suitable additives for bricks production: Kieselguhr sludge et al., (2006), organic residues
84 (Demir, 2008), granite and marble wastes (Dhanapandian and Gnanavel, 2009), spent shea
85 waste (Adazabra et al., 2017a,b), wastewater sludge (Jianu et al., 2018), coal fly ash (Eliche-
86 Quesada et al., 2018), degraded municipal solid waste (Goel and Kalamdhad, 2017), waste
87 glass sludge (Kazmi et al., 2018), cotton soils (Zhang et al., 2013), quarrying wastes
88 (Rukijkanpanich and Thongchai, 2019), bricks kiln dust (Riaz et al., 2019), shale, sewage
89 sludge, coal gangue powder and iron ore tailings (Luo et al., 2020) and electrolytic
90 manganese residue (Li et al., 2020) which are exciting and suitable additives for bricks
91 production.

92 To the knowledge of the authors, no paper was published dealing with the use of
93 sludge from the inert mineral part of the construction and demolition waste sludge (RA-S) for
94 manufacturing of fired bricks. This waste is usually generated into wastewater treatment
95 plants through washing processes that are essential for the recycling of waste concrete as
96 aggregate materials. Washing removes clay, silt, sand, mortar, and other fine particles, which
97 improves the quality of aggregates for subsequent processing. A considerable amount of

98 wastewaters can also come through the wet crushing of construction and demolition wastes
99 (CDW) (Yoo et al., 2018). The wet-based crushing process is commonly applied to remove
100 impurities and to wash the concrete surface and reduce air pollution (Yoo et al., 2018; Behera
101 et al., 2014). During these processes, a significant amount of sludge can be generated. This
102 sludge presents fine particles and high moisture content, nearly 93 wt% (Yoo et al.,
103 2018; Behera et al., 2014). The sludge is submitted to flocculation, solids precipitation and
104 dewatering in press-filters to optimize the solid/liquid separation. By this process, the
105 moisture content is decreased to about 30 wt%.

106 The brick quality depends mainly on the waste composition (concrete, masonry,
107 bricks, roads, and others), which in its turn also depends on its generation source (Murmu
108 and Patel, 2018). In addition to the properties of the materials, the quality of the fired bricks
109 also depends on the fabrication method, drying procedure, and firing process (Velasco et al.,
110 2014). These factors will affect the properties of the final product, such as compressive
111 strength, water absorption, impact and abrasion, tensile strength, and others. (Murmu and
112 Patel, 2018; Zhang et al., 2017). Bricks with high quality present high compressive strength
113 and low water absorption. Compressive strength is profoundly affected by firing temperature,
114 method of production and physical, chemical and mineralogical properties of the raw material
115 (Bruno et al., 2019; Karaman et al., 2006; Mbumbia and de Wilmars, 2002).

116 In this study, for the first time, it was explored the applicability of RA-S from
117 wastewater treatment plant as the primary raw material for fired bricks fabrication. The focus
118 of this study is to investigate the physical and chemical properties of the fired bricks by
119 incorporation of RA-S as the main additive and to explore their thermal characteristics. For
120 this purpose, bricks fabricated with different dosages of RA-S and earth material (i.e., 0%,
121 30%, 50%, 70% and 100% by weight) were prepared and evaluated in terms of their
122 properties. Utilization of RA-S in manufacturing fired bricks can be a helpful approach in
123 reducing issues related to the landfill process and in solving environmental problems
124 associated with RA-S management. Moreover, fired bricks with good and acceptable
125 features can be fabricated even at the industrial scale, which leads to more sustainable and
126 economical construction activities.

127

128 **2. Materials and Methods**

129

130 *2.1. Raw materials*

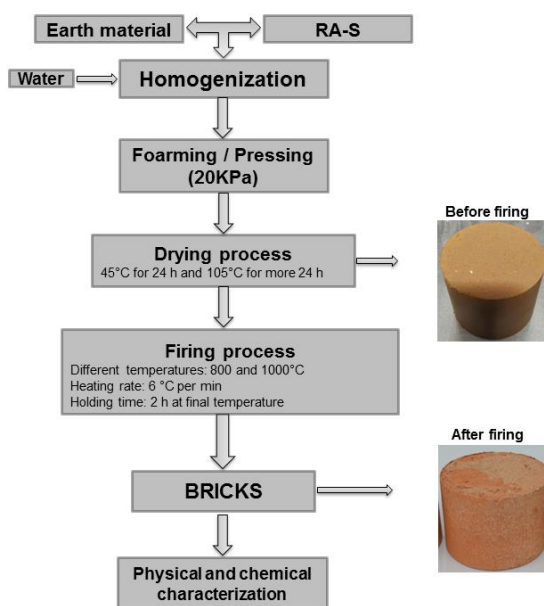
131 The RA-S sample used in this study was collected from a recycling demolition and
132 construction waste plant in Frejus, south of France. The sample was collected after be
133 passed by the press filter, its initial moisture was around 32%. The moisture content of the
134 RA-S was determined based on oven-drying at 105°C until there was no change in weight.

135 The samples were ground and completely sealed to prevent a decrease in pH and Ca
 136 concentration in solution via natural CaCO₃ precipitation between Ca and atmospheric CO₂.

137

138 **2.2. Preparation of fired bricks**

139 The Earth material and RA-S raw materials were blended to produce homogenous
 140 mixtures containing 20 wt% water with adequate plasticity. The mixtures were made with the
 141 following mass proportions of RA-S in the total dry mixture: 0%, 30%, 50%, 70%, and 100%.
 142 The bricks were named according to the amount of each raw material and their firing
 143 temperatures (see **Table 1**). Also, brick preparation is highlighted in **scheme 1**.



144

145 **Scheme 1**– Fluxogram for brick preparation.

146

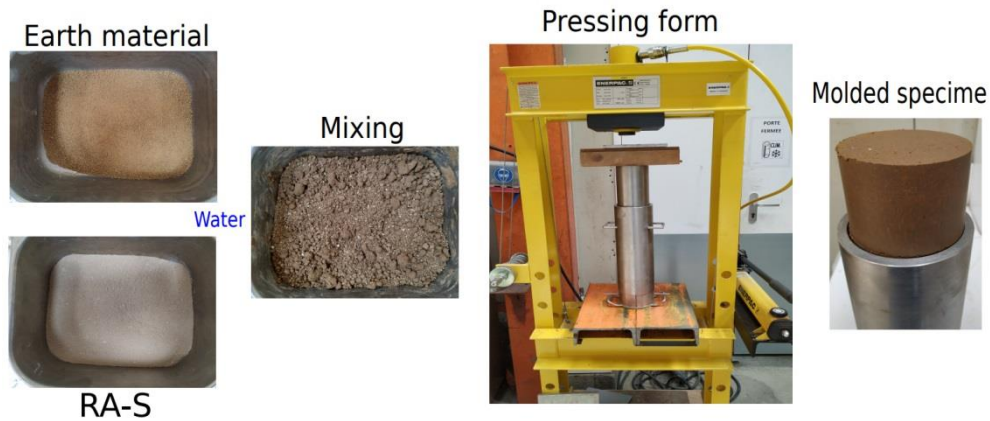
147 **Table 1** - Proportion of the mixtures earth material, RA-S, and water amounts in the different
 148 brick mixture (the amount is given for one brick).

| Samples name | RA-S (kg) | Earth material (kg) | Water (kg) |
|------------------------------|-----------|---------------------|------------|
| 100% Earth material 800°C | 0 | 1.0 | 0.2 |
| 100% RA-S800°C | 1.00 | 0 | 0.2 |
| 30% RA-S800°C | 0.3 | 0.7 | 0.2 |
| 50% RA-S800°C | 0.5 | 0.5 | 0.2 |
| 70% RA-S800°C | 0.7 | 0.3 | 0.2 |
| 100% Earth material1000°C | 0 | 1.0 | 0.2 |
| 100% RA-S1000°C | 1.00 | 0 | 0.2 |
| 30% RA-S1000°C | 0.3 | 0.7 | 0.2 |
| 50% RA-S1000°C | 0.5 | 0.5 | 0.2 |
| 70% RA-S1000°C | 0.7 | 0.3 | 0.2 |

149

150 *2.2.1. Forming*

151 Fired brick specimens were formed using an extrusion process (see Fig. 1). The
152 bricks mold were made with 1 kg of dried raw materials plus 20 wt% of moisture; the molding
153 process is highlighted in Fig. 1. All the brick specimens were compacted with the same force
154 in a mold of 100 mm diameter and 75 mm height, with a compaction force of 20 - 22 kN.
155 Afterward, the brick samples were dried at 40°C in an oven for 24 h, followed by 24h at
156 105°C (see scheme 1).



157
158 **Fig. 1**–Molding process of the prepared bricks.

159
160 *2.2.2. Firing process*

161 Dried brick samples were fired in a laboratory electric furnace with a heating rate of
162 6°C/min, and dwelled for 2 h at the maximum temperatures 800 and 1000°C; afterwards, the
163 furnace was shut down, and the fired bricks were cooled down inside the furnace until room
164 temperature was reached (see scheme 1).

165
166 *2.3. Microstructure and chemical characteristics of the raw material and fired bricks*

167 The chemical composition of the raw materials (RA-Sand earth material) and fired
168 bricks were analyzed by X-ray fluorescence (XRF) and wavelength Dispersive (WD-XRF). X-
169 ray diffraction (XRD) was also employed to evaluate the mineralogical composition of the raw
170 materials and fired bricks.

171 Scanning Electron Microscopy (SEM) was used to observe microstructures of both
172 raw materials and fired bricks by using an electron microscope JEOL (model SM 840). The
173 samples were metalized with gold by using an ion sputtering device JEOL (model JFC 1100)
174 to obtain the SEM images. The functional groups of the raw materials and fired bricks were
175 determined using Fourier Transform Infra-Red Spectroscopy (FTIR) (LAMBDA 365 UV/Vis
176 Spectrophotometer) with the ATR (Attenuated Total Reflectance) accessory. The spectra
177 were recorded with 64 cumulative scans over the range of 4000–400 cm⁻¹ with a resolution of
178 4 cm⁻¹.

179

180 2.4. Physical and geotechnical properties of the raw materials and fired bricks

181 The grain size distribution of both raw materials was determined by the standard of
182 sedimentation (NF P 94057) to determine the size of the particles under 0.08 mm. Moreover,
183 for particles size upper 0.08 mm it was used dry sieving standard NF P 94056. The Atterberg
184 limits of the fine fraction were determined according to the norm NF P94-051 (AFNOR,
185 1993). Linear shrinkage was determined through the difference between the diameter of the
186 dry and fired specimens divided by the diameter of the dried sample (Ukwatta et al.,
187 2017).The loss of ignition (LOI) of the RA-S and earth material was determined by calcination
188 at 1000°C for 2 h (Eliche-Quesada et al., 2018). Weight loss data of fired bricks were
189 obtained by the difference between the weight after drying and firing processes (Eliche-
190 Quesada et al., 2018).The thermal conductivity of raw materials and fired bricks were
191 measured by the hot plate method, according to Poullain et al. (2006).

192

193 3. Results and discussion

194

195 3.1. Particle size distribution of the RA-S

196

197 The particle size distributions of RA-S and earth material are shown in **Fig. 2**.
198 Significant presences of particles of medium and fines sizes were observed. The particle
199 sizes of the RA-S are finer than those of the earth material. The mean particle size, D50, was
200 0.012 mm for the RA-S (red line), whereas for the earth material the D50 was of 0.19 mm
201 (blue line) (See Fig.2). RA-S is made up mainly of particles of the size of clay and silt
202 followed by the sand in terms of percentage (see Table 2).

203

204 Table 2 - Physical characteristics of the RA-S and Earth material

| Characteristics | RA-S | Earth material |
|--|-------|----------------|
| Clay content (%) | 22 | 33.0 |
| Silt content (%) | 56 | 31.0 |
| Sand content (%) | 23 | 32.2 |
| Density (kg cm ⁻³) | 2.66 | 2.66 |
| PL (%) | 28.7 | 23.5 |
| LL (%) | 46.77 | 51.3 |
| PI | 18.07 | 27.8 |
| Loss on ignition (%) | 18.04 | 6.35 |
| Thermal conductivity (W.m ⁻¹ .K ⁻¹) | 0.093 | 0.181 |

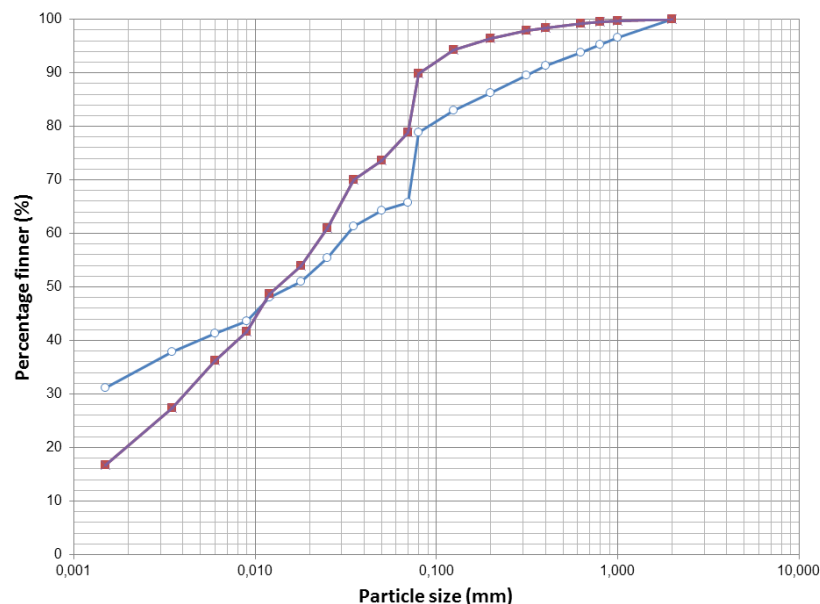
205

206 The finest particles (size distribution) might help in the brick quality in terms of
207 physical and chemical properties due to two main reasons: (i) provide filling and the
208 formation of a compact structure with suitable particle size distribution; and (ii) can increase
209 the plasticity of the material when it is moistened (Leonel et al., 2017; Vieira and Monteiro,

210 2006). This could be attributed to the higher surface area of the finer particle that can provide
211 better mixing among both RA-S and earth material. When coarser material is mixed with finer
212 particles, the pores and spaces between coarser particles are filled up with finer particles (Hir
213 et al., 2011). This provides stronger consolidation with the earth material, consolidation is
214 characterized by the formation of inter-particle interactions; it describes the ability of a
215 powder bed to form mechanically durable bonds with sufficient strength (Grossmann et la.,
216 2004). Besides, it was observed that the pozzolanic activity increases when the specific
217 surface of the particles increases (Agarwal, 2006).

218 Kazmi et al. (2017a, 2017b) demonstrated that the performance of fired bricks could
219 be affected by the particle size distribution and by the production origin of the raw materials.

220



221

222 **Fig. 2-** Grading curves of earth material and RA-S. (Blue line = RA-S and red line = earth
223 material).

224

225 3.2. Plasticity of the RA-S

226 Plasticity is a valuable property that allows a specific material to form a plastic body.
227 This property needs to be evaluated in brick fabrication (Murray, 1991). Low plasticity may
228 cause heterogeneities in the molding mass, which reflects weak mechanical
229 properties(Murray, 1991). Besides, the plasticity of clay or any material also depends on their
230 particle-size distribution (Murray, 1991). Mixtures with finer particles may have better
231 plasticity than larger particles due to the higher surface area and consequently, stronger
232 cohesive forces (Murray, 1991).

233 The Atterberg limit test was performed to determine the plasticity characteristic of the
234 RA-S. By this test, it was possible to obtain the liquid limit (LL), plastic limit (PL), and
235 plasticity index (PI). The RA-S presented a LL of 46.77%, a PL of 28.7% and a PI of 18.07%.
236 Such results classify the RA-S as an inorganic material with high plasticity according to the
237 Unified Soil Classification System USCS ASTM D2487-11 (2011), (see Table 2).

238 Comparing to the literature, Kazmi et al. (2018) prepared good quality fired bricks by
239 incorporating marble sludge. A liquid limit of 26.1% and a plasticity index of 7.4%. Sarani et
240 al. (2018) prepared fired bricks with earth material, and their LL and plasticity index
241 was 28.7% and 13.4%, respectively, which meet technical recommendations. Good brick
242 material must have an ideal Atterberg limit value in the range of 12% to 22% (plastic limit)
243 and 7% to 18% (plasticity index) (Sarani et al., 2018). It is essential to say that the RA-S
244 used in this study presents an important degree of plasticity (within the technical
245 recommendations), which makes it a promising waste material for brick fabrication.

246

247 3.3. XRF Characterization

248

249 The chemical composition of the RA-S, earth material and fired bricks were
250 determined by XRF. The results are shown in **Table 3**. The earth material displayed a typical
251 composition and mainly consisted of Silica (SiO_2), Alumina (Al_2O_3), and Ferric Oxide (Fe_2O_3),
252 and other oxides present in trace amounts, such as K_2O , MgO , P_2O_5 , and TiO_2 (see **Table 3**).

253 RA-S is mainly formed by SiO_2 , Al_2O_3 , CaO , and ferric oxide, with small amounts of
254 MgO , K_2O , P_2O_5 , and TiO_2 (see **Table 3**). The oxides, such as K_2O , Na_2O , Fe_2O_3 , CaO
255 (10.3%) and MgO can promote better vitrification and may increase the densification of the
256 fired bricks during the heating process (Eliche-Quesada et al., 2018).

257 As can be seen in **Table 3**, the amount of SiO_2 , Al_2O_3 , and Fe_2O_3 , in the bricks,
258 decreased as the amount of the RA-S increased. This is because the RA-S contains lower
259 amounts of alumina and silica compared to the earth material. On the other hand, the CaO
260 content is higher in the samples with higher RA-S content, due to the presence of carbonates
261 from concrete matrixes.

262 In general, raw materials with high silica content (e.g., higher than 60%) are not
263 recommended for the preparation of fired bricks because they destroy the cohesion between
264 particles so that the brick becomes brittle (Kazmi et al., 2017a,b). However, the silica content
265 in the RA-S is lower than in the earth material (see **Table 3**), and this might not negatively
266 affect the quality of the fired bricks when both are mixed.

267 The earth material presented 0.1% CaO , while RA-S presented 10.17% CaO . The
268 presence of CaO might be benefic for manufacturing clay bricks. Rukijkanpanich and
269 Thongchai, (2019) used quarrying wastes with high CaO content (26.50%) for fired brick

270 fabrication. They concluded that CaO was benefic for the brick qualities; also, they
 271 highlighted that the presence of CaO was responsible for decreasing both porosity and the
 272 water absorption as the effect of sintering process between CaO and SiO₂ which also
 273 resulted in the higher compressive strength. In light of these results, based on its chemical
 274 composition, it is possible to infer that RA-S is a promising raw material for brick
 275 manufacturing.

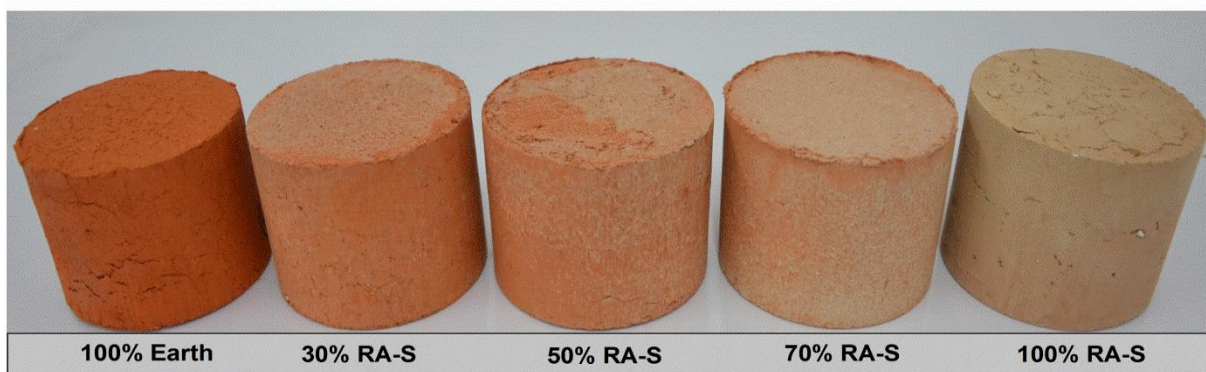
276 Fe₂O₃ is a good influence for the aesthetic of the bricks samples since higher iron
 277 oxide contents result in a stronger red colour (see **Fig. 3**). The blend (RA-S + earth material)
 278 provoked changes in the red color (depending on the amount blended).

279

280 **Table 3** - The chemical composition of the RA-S, Earth material, and bricks fired at 800°C
 281 expressed in their oxides.

| Oxides (%) | RA-S | Earth material | 0% RA-S | 30% RA-S | 50% RA-S | 70% RA-S | 100% RA-S |
|--------------------------------|-------|----------------|---------|----------|----------|----------|-----------|
| SiO ₂ | 40.55 | 54.5 | 52.3 | 50.6 | 48.8 | 48.1 | 44.6 |
| Al ₂ O ₃ | 12.9 | 26.8 | 26.5 | 22.8 | 21.5 | 20.4 | 18.2 |
| CaO | 10.17 | 0.1 | 0.3 | 4.0 | 9.1 | 9.8 | 10.1 |
| Fe ₂ O ₃ | 4.02 | 12.6 | 15.5 | 12.8 | 9.7 | 8.7 | 9.6 |
| K ₂ O | 2.57 | 3.0 | 2.4 | 3.2 | 3.3 | 3.3 | 3.7 |
| MgO | 1.8 | 0.4 | 0.5 | 1.0 | 1.8 | 2.1 | 3.6 |
| Na ₂ O | 1.2 | 0.5 | 0.6 | 0.6 | 1.3 | 1.4 | 1.6 |
| SO ₃ | 2.58 | 1.3 | 0.9 | 2.1 | 2.5 | 2.9 | 3.6 |
| TiO ₂ | 0.44 | 1.0 | 1.0 | 1.1 | 1.2 | 0.9 | 1.0 |
| P ₂ O ₅ | 0.1 | - | - | - | - | - | - |

282



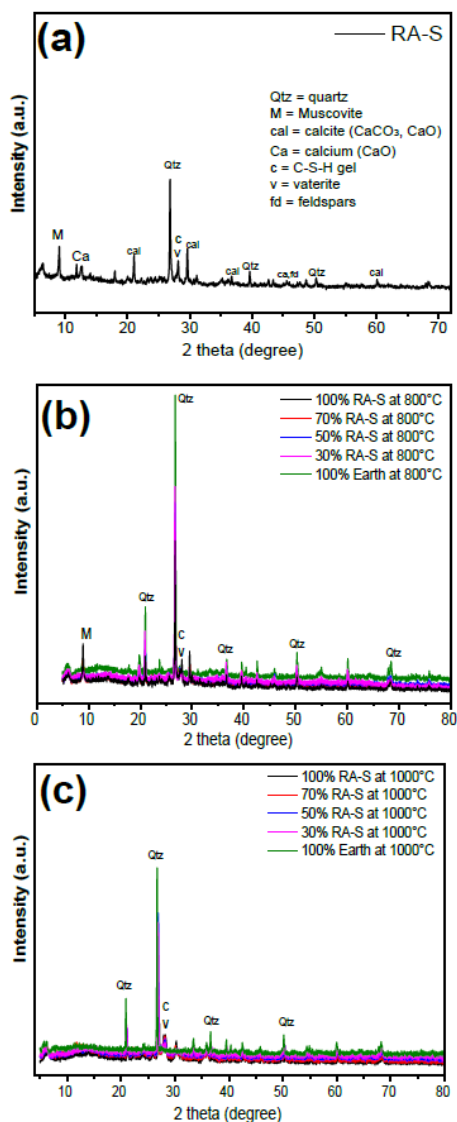
283
 284

Fig. 3- Appearance of then fired brick at 800°C. (Sectional view).

285

286 3.4. XRD characterization

287 In brick fabrication, the identification of the main mineral/crystalline phases present in
 288 the raw material and in the final product represent an aspect of significant importance. In this
 289 matter, XRD allows accurate information regarding the crystalline phases of the bricks and
 290 their original raw material (Moreno-Pérez et al., 2018). Fig. 4 shows the typical XRD patterns
 291 of the RA-S and different fired bricks. According to the images, there are some changes in
 292 the XRD patterns between the RA-S and bricks. Comparing the XRD patterns, we can
 293 observe that the intensity in the crystallinity peaks was higher in samples with higher earth
 294 material content as well as for samples fired at 800°C when compared to 1000°C.



295
 296 **Fig. 4** - XRD patterns of (a) RA-S; (b) fired bricks at 800°C and (c) fired bricks at 1000°C.

297
 298 According to the **Fig. 4a**, the mineralogy properties of RA-S indicate the presence of
 299 a crystalline phase composed mainly by quartz (SiO_2), alumina, calcite (CaCO_3) and calcium
 300 (CaO , $\text{Ca}(\text{OH})_2$), among others (Yoo et al., 2018). The intense aluminosilicates (silicon

301 dioxide and kaolinite) peaks show them as the main constituents of the earth material,
302 which aligns with XRF results (Table 3). The presence of muscovite ($KAl_2(Si_3AlO_{10})(OH)_2$)
303 was also identified in the RA-S (Fig. 4a). Muscovite presented in these bricks is originated
304 from cement/mortar (Yoo et al., 2018). The calcite is formed via the natural carbonation of
305 lime (CaO) with atmospheric CO_2 (Mo et al., 2017).

306 When comparing the firing temperature (see Fig. 4b and c), some changes are
307 observed; it seems that most of the peaks are higher in the bricks fired at 800°C and diminish
308 when the bricks are fired at 1000°C. The microstructure of the bricks fired at 800°C
309 presented higher peaks compared to bricks fired at 1000°C (see Fig. 4b and c), and this
310 could reflect in the physical characteristics of the bricks fired at 800°C.

311 The mineralogy composition of RA-S supports its reuse in the brick
312 fabrication because the vast diversity of inorganic oxides presence could be advantageous to
313 decrease the melting point of the mixtures (earth material+ RA-S) during sintering (Chen et
314 al., 2013).

315

316 *3.5. FTIR of the raw materials and fired bricks*

317 FTIR was carried out to identify the presence of functional groups on the surface of
318 the materials, which permits further observations and understanding about surface features
319 of the raw materials and fired bricks.

320 In the spectra of the earth material and RA-S (Fig. 5a) are presented different peaks at
321 3621 cm^{-1} , which was found only in earth material (that could be assigned to hydroxyl groups
322 present in smectite and bentonite) (Djomgoue and Njopwouo, 2013). Also, at 1437 cm^{-1} it
323 was found only in RA-S, which could be attributed to the symmetrical and asymmetric modes
324 of vibration of the $(CO_3)^{2-}$ (Eliche-Quesada et al., 2018). The results confirm the presence of
325 carbonates that is in agreement with the previous XRD and XFR analysis.

326 Fig. 5B highlights the peaks of both raw materials below 1000 cm^{-1} . The peaks (in both
327 samples) at the region between 1000 and 909 cm^{-1} could be assigned to the SiO_2 stretching
328 modes that come from the aluminosilicates in both samples but for the RA-S could also come
329 from CSH gel (Eliche-Quesada et al., 2018). The peak at 872 cm^{-1} is observed only in the
330 RA-S (see Fig. 5b) is assigned to the carbonate flexion vibration (Eliche-Quesada et al.,
331 2018).

332

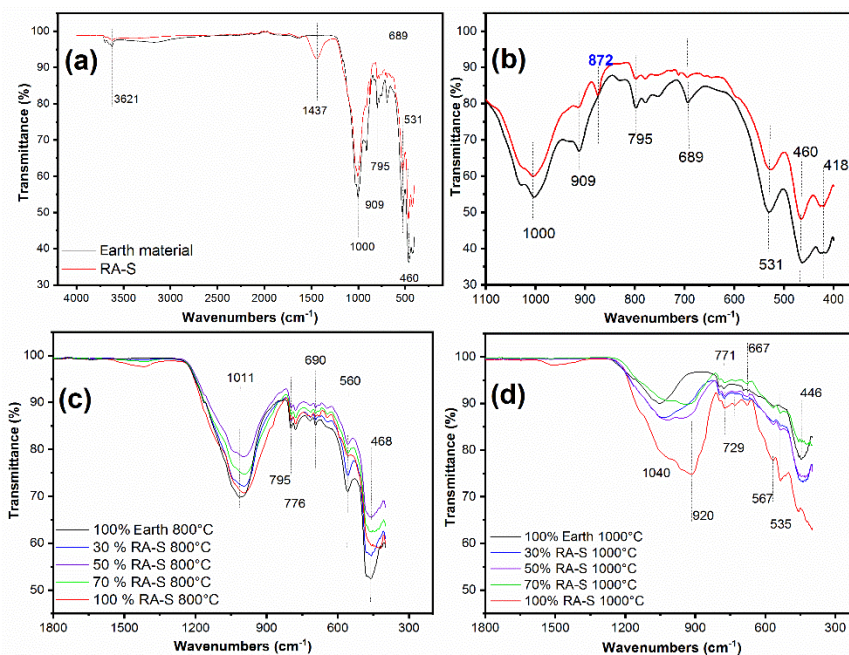


Fig. 5 - FTIR spectra of (a) raw materials; (b) Peaks below 1000 cm^{-1} for both raw materials; (c) Fired bricks at $800\text{ }^{\circ}\text{C}$; and (d) fired bricks at $1000\text{ }^{\circ}\text{C}$.

333
334
335
336

337 Comparing FTIR results of the raw materials (Fig. 5a and b) and fired bricks (Fig. 5c
338 and d), it was observed that the peak found in 3621 cm^{-1} disappeared in all fired bricks
339 (results not shown). RA-S displayed a band at 1437 cm^{-1} , which is ascribed to the stretching
340 vibration of O-C-O (due to the presence of carbonates) (Zhang et al., 2015), this band was
341 not present in earth material. After firing the bricks this band also disappeared in all bricks;
342 carbonates is decomposed around $600\text{-}800^{\circ}\text{C}$ (Zhang et al., 2015).

343 To observe it in more detail, the FTIR spectra of the fired bricks are shown in the
344 interval from $200\text{ to }1800\text{ cm}^{-1}$ (see Fig. 5c and d). In Fig. 5c it is observed that the firing
345 temperature at 800°C did not cause significant differences in the IR spectra, only in their
346 intensities.

347 In addition, by analyzing the effect of temperature over the presence of surface
348 groups, it can be seen that the bricks fired at 1000°C exhibited lower intensity and broader
349 peaks in comparison to the bricks fired at 800°C (see Fig. 5c and d), highlighting that the
350 firing process affected the presence of functional groups on brick surfaces. It can be inferred
351 that at 1000°C the functional groups were lost provoked by the higher temperature and that
352 can have effects on the fired bricks final properties. The loss of chemical elements could
353 imply less strength of the brick structure.

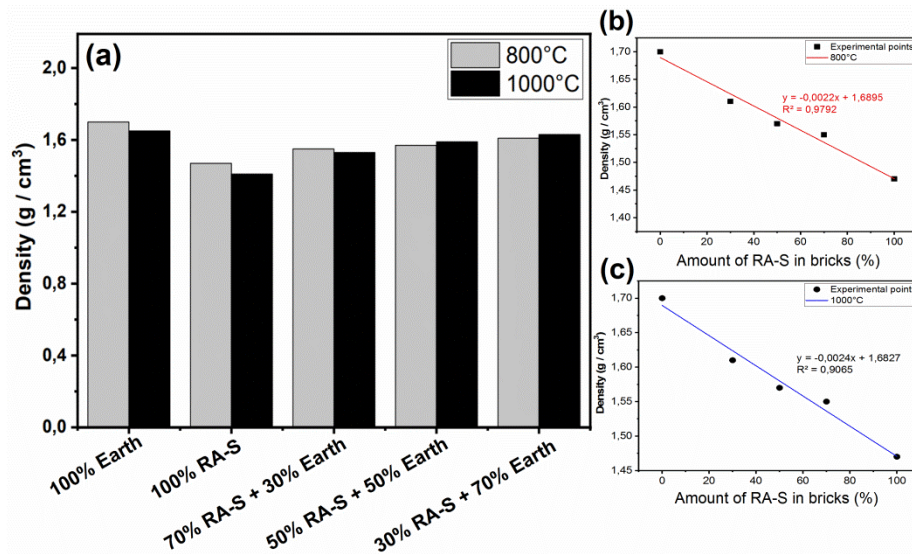
354 Further analyzing the brick surface, it is observed the presence of quartz in 771 and
355 776 cm^{-1} , which could be attributed to Si-O symmetrical stretching vibrations whereas
356 around $667\text{ - }690\text{ cm}^{-1}$ might be assigned to Si-O symmetrical bending vibrations due to the
357 low level of Al for Si substitution (Viruthagiri et al., 2015).

358
359
360
361
362
363
364
365
366
367
368
369
370
371
372
373
374

3.6. Bulk density

Fig. 6 shows the density for different compositions of the bricks fired at 800 and 1000°C. As denoted in Fig. 6, the density values were slightly influenced by the quantity of RA-S added. The pure earth brick and pure RA-S brick presented substantial differences in their density values, 1.7 and 1.65 g/cm³ for 100% earth and 1.47 and 1.41 g/cm³ for the 100% RA-S fired at 800 and 1000°C, respectively; densities 13.5% and 14.5% higher for the fired bricks made with 100% of Earth material in comparison with the bricks made with 100% RA-S.

Besides, it is observed that the density for the bricks with 30, 50, and 70% of RA-S narrowly varied. The values were slightly lower for the bricks made higher RA-S amounts, 1.61, 1.57 and 1.55 g/cm³ were observed for those bricks made with 30, 50 and 70% of RA-S (and burnt at 800°C), respectively. The same trend was observed for the brick samples fired at 1000°C (see Fig. 6). In general, an increase in the RA-S content led to a slight decreasing in the bulk density of the fired bricks. It suggests that the microstructure of the bricks (RA-S + Earth material) played a role in their physical properties.



375
376 **Fig. 6** - (a) Density of the fired bricks as a function of waste addition and (b) relationship
377 between density and RA-S addition in the fired bricks.
378

379 In terms of temperature effect, it seems that the firing temperature did not cause
380 significant effects on the bulk density of the bricks. The results show that increasing the
381 temperature resulted in a slightly decrease on the brick densities.

382 There seems to be a good correlation between the RA-S content and brick density at
383 both temperatures, $R^2=0.9792$ and 0.9065 for 800 and 1000°C, respectively. However, other

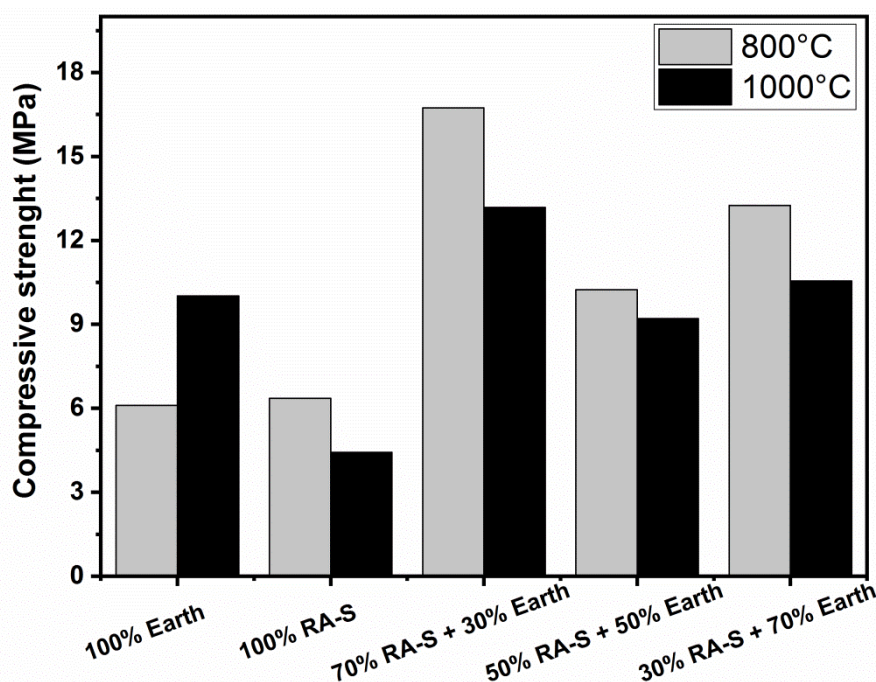
384 factors as mineralogical composition, microstructure, and pressing method of the bricks are
385 essential factors that affect the density of the bricks.

386

387 3.7. Compressive strength of the bricks

388
389 The compressive strength (CS) is highly important in terms of engineering quality of
390 the fired bricks since it measures the ability of bricks or any material to withstand loads. The
391 CS of the fired bricks was measured according to the French Standards (AS/NZS 4456,
392 2003). Fig. 7 shows the compressive strength results of burnt bricks incorporating with RA-S.
393 The results in Fig. 7 show that the fabricated brick made with 70% sludge and 30% earth
394 material and burnt at 800°C presented the highest CS of 16.8 MPa. Interestingly, the bricks
395 made with a high amount of RA-S showed higher CS values, which is much higher than the
396 minimum requirement for compressive strength recommended by many Standards (see
397 **Table 4**). For instance, a minimum compressive strength of 3.0 MPa is recommended
398 according to the Australian Standards. The Brazilian standard recommends a minimum
399 compressive strength of 1.5Mpa.

400



401

402 **Fig. 7 - Compressive strength of the fired bricks at 800 and 1000°C.**

403

404 According to Fig. 7, the results show that CS is dependent on the firing temperature.
405 CS values for the samples fired at 800°C reached higher CS when compared with samples
406 burned at 1000°C. An exception was for the brick made with 100% earth material that
407 presented higher CS for the sample fired at 1000°C. The CS of the fired bricks increased

408 with the addition of the RA-S for both temperatures. According to the many standards, the
 409 values of CS are still higher when compared to the values presented in **Table 4**.

410

411 **Table 4** - Standard minimum compressive strength requirement as per different standar

| International standard | Brick classification | Minimum compressive strength (MPa) | Code (reference) |
|--------------------------|---|------------------------------------|-----------------------------|
| Brazilian Standard | Clay bricks | 1.5 | NBR 6064 (ABNT 1983a) |
| China National Standard | First degree Second degree Third-degree Pavement bricks | 14.71 9.81 7.35 49.03 | CNS382:R2002, 2007 |
| Building bricks | Severe weathering Moderate Weathering Negligible Weathering | 20.7 17.2 10.3 | ASTM C62 – 13a, 2013 |
| Solid Masonry Unit | Vertical coring Horizontal coring | 20.7 13.8 | ASTM C126 – 16, 2011 |
| Hollow concrete blocks | Grade A Grade B Grade C | 3.5–15 3.5–5 4–5 | IS 2185-1, 2005 |
| Common burnt clay bricks | Burnt clay bricks | 3.5–35 | IS1077, 2007 |
| Hollow clay bricks | Hollow bricks | 3.5 | IS3952, 2006 |
| Concrete masonry units | Hollow load-bearing Grade A Hollow load-bearing Grade B Hollow non-load bearing Solid load-bearing Grade A Solid load-bearing Grade B | 5.5 4 3.5 10.8 7 | IS 2185-2, 1983 |
| Facing bricks | Severe weathering Moderate weathering | 20.7 17.2 | ASTM C216-07a |
| Concrete Block | - | 11.6 down to 2.1 | Standard (TZS 283,2002 (E)) |

412 See reference (Murmu and Patel, 2018)

413

414 As can be seen in Fig. 7, CS of fired brick follows a pattern about the ratio RA-S/Earth
 415 material. A minimum compressive strength was observed for the bricks with 100% of RA-S:
 416 4.4 and 6.3 MPa for both temperatures 1000 and 800°C, respectively. The pure earth
 417 material generated bricks with 6.1MPa and 10.0MPa for 800 and 1000°C, respectively.

418 At the temperature of 800°C, the control brick (100% of earth material) presented 6.1
 419 MPa (seen Fig. 7). In addition, in relation to the control brick, bricks made by incorporating
 420 30%, 50% and 70% RA-S increased their CS in 67.6%, 116.9% and 173.8%, respectively;
 421 their CS were 10.2 MPa, 13.2 MPa, and 16.7 MPa after incorporating 30%, 50% and 70%
 422 RA-S, respectively. For the bricks fired at 1000°C, the control brick presented a CS of 10.0
 423 MPa, 38.9% higher than the sample fired at 800°C. However, when RA-S was added, the CS

424 increased with the increasing of the RA-S amount in the fired bricks (at 1000°C). Exhibiting the
425 same behavior presented by bricks fired at 800°C (See Fig. 7).

426 Kazmi et al. (2018) observed similar results after adding waste glass sludge in clay
427 bricks. The authors found that the lowest CS was observed for control bricks; and that
428 increasing the amount of waste in the bricks led to higher CS values. The same behavior
429 was related by Chidiac and Federico (2007) after adding waste glass into fired bricks. For
430 fired bricks, CS is strongly influenced by the characteristics of the raw materials that they are
431 made as well as by the production process.

432 In addition, CS is also related to the density. Generally, there is a clear positive
433 correlation between compressive strength and density. However, in this investigation, the
434 addition of RA-S did not cause big influences on the CS. The same behavior was related by
435 Mubiayi et al. (2018) after preparing fired bricks by incorporating jarosite, clay and fly ash. It
436 was found no correlation between CS and density. Maza-Ignacio et al., (2020) prepared fired
437 bricks from sugarcane bagasse ash and demonstrated that the bricks with the highest CS did
438 not present the highest densities. The same results were found by Eliche-Quesada et al.,
439 (2018). Sarani et al, (2018) produced fired bricks by incorporating mosaic sludge and
440 showed that the dry density of manufactured bricks decreased while the compressive
441 strength increased. The development of microstructure inside the brick body could provoke
442 such trend (Sarani et al, 2018).

443 Besides, the combination of the RA-S and earth material could be responsible for the
444 mechanical resistance increasing of the fired bricks in detriment of the bricks made only with
445 the raw materials. For instance, the brick made with 70% of RA-S and fired at 800°C
446 presented the highest CS and but not the highest density. A possible explanation could be
447 due the mixing and molding processes between RA-S and earth material; as previously
448 discussed in section 3.1, it was highlighted that the finer particles of RA-S filled up the pores
449 and spaces of the coarser particles of earth material which provided stronger consolidation
450 between the brick particles to form mechanically durable bonds with sufficient strength
451 (Grossmann et la., 2004).

452 This statement will be corroborated by SEM images that showed a more cohesive
453 microstructure of the brick made with 70% of RA-S and 30% of earth material when
454 compared to the other bricks (See Fig. 10 and its discussion).

455

456 *3.8. Firing shrinkage of fired bricks*

457 Bricks exhibit a variation in their dimensions due to shrinkage during both drying and
458 firing processes, reflecting the expansion/contraction behavior during the drying and firing
459 treatment. The firing shrinkage of the fired bricks was found to increase with the addition of

460 RA-S, as shown in **Table 5**. The firing shrinkage of the fired brick with RA-S showed little
 461 expansion behavior (see **Table 5**).

462 However, the bricks made with pure earth material presented contraction behaviors
 463 (0.61 and 0.95% for the bricks fired at 800 and 1000°C, respectively). These contractions
 464 were probably caused by the vitrification process, which forms glassy layers in the ceramic
 465 body during the heating process resulting in bonding earth particles together (Eliche-
 466 Quesada et al., 2018; Dizhur et al., 2016). These findings are in accordance with the density
 467 results which showed that the bricks made with pure earth material have the highest density
 468 values (see Fig. 6).

469 The results suggest that the increment of the RA-S in the fired bricks slightly
 470 increased their expansions (See Table 5). These findings are following Ukwatta and co-
 471 workers (2017) that incorporated biosolids in fired bricks and found the same behavior, an
 472 expansion in the brick dimensions with the amount of waste added. Eliche-Quesada et al.
 473 (2018) also observed the same behavior.

474

475 **Table 5** - Linear shrinkage of the fired bricks

| Fired Bricks | Firing shrinkage (%) |
|----------------------------|-----------------------------|
| 100% Earth material 800°C | (-)0,61 |
| 100% RA-S 800°C | (+)0,55 |
| 30% RA-S 800°C | (+)0,12 |
| 50% RA-S 800°C | (+)0,47 |
| 70% RA-S 800°C | (+)0,28 |
| 100% Earth material 1000°C | (-)0,951 |
| 100% RA-S 1000°C | (+)0,228 |
| 30% RA-S 1000°C | (-)0,091 |
| 50% RA-S 1000°C | (+)0,036 |
| 70% RA-S 1000°C | (+)0,27 |

476

477 In general, the RA-S additions did not provoke significant changes in the linear
 478 shrinkage of the brick bodies which is a good indicative since high shrinkage causes
 479 destruction of the bricks in firing and drying stages of production. Therefore, RA-S is a
 480 promising additive (in terms of shrinkage prevention) for brick fabrications since it remains
 481 the brick bodies stable even during firing processes at 800 and 1000°C.

482

483 *3.9. Loss on ignition (LOI) and Heat Loss*

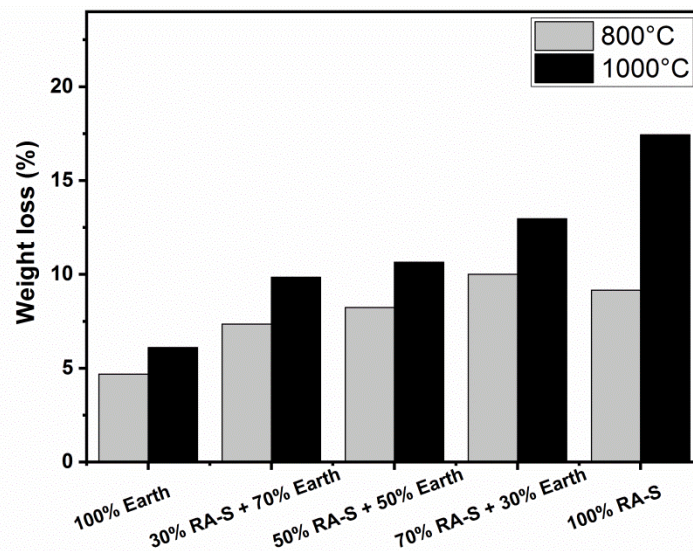
484 LOI is a simple method for estimating the content of organic matter and carbonate
 485 minerals present in the materials (Dean, 1974). Organic matter initiates ignition in
 486 temperatures around 200 °C, and it is completely burnt in temperatures around 550°C.
 487 Minerals such as carbonates are entirely depleted at higher temperatures (around 800 –
 488 850°C) (Santisteban et al., 2004).

489 As seen in Table 2, the LOI is higher in RA-S (18.4%) compared to earth material
490 (6.35%). The LOI value of 18.4 wt% indicates a higher content of burnt elements. This makes
491 sense since the composition of RA-S has a higher amount CaO (10.17%) in comparison to
492 earth material (0.1%) (See Table 3) and this could explain the higher LOI value (Eliche-
493 Quesada et al., 2018).

494 Depending on the firing process, the weight loss of fired bricks can intensively vary.
495 As expected, by increasing the firing temperature from 800 to 1000°C, the weight loss of the
496 brick also increased (see Fig. 8).

497 The higher addition of RA-S increased the weight loss of the fired bricks at both
498 temperatures (see Fig. 8). The weight loss might be attributed, mainly, to the dehydroxylation
499 processes of the silicates and the decomposition of the carbonates (Eliche-Quesada et al.,
500 2018).

501



502

503

Fig. 8– Weight loss of fired bricks.

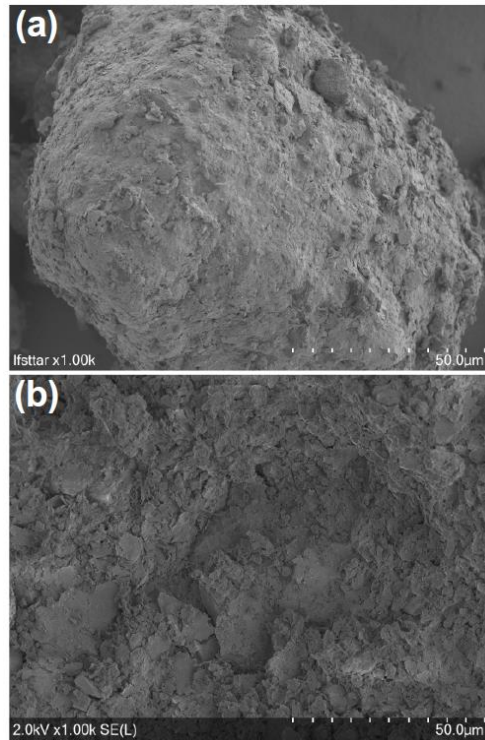
504

3.10. Microstructure analysis of the raw materials and fired brick

505

506 Scanning electron microscopy (SEM) is one of the main techniques for material
507 characterization due to its ability to provide morphological and structural details of different
508 materials. Fig. 9 presents microstructure images of Earth material and RA-S provided by
509 SEM. The images revealed remarkable differences in the microstructures. The earth material
510 showed irregularly shaped particles with different sizes (coarser than RA-S), as well as rough
511 texture. RA-S exhibits very fine agglomerated layered structures (See Fig. 9b).

512 The agglomeration of the RA-S may help in increasing the density of the bricks
513 because it can reduce the pore spaces in the brick matrix during molding and pressing
514 processes, which reflects in good mechanical strengths (Celary and Sobik-Szoltyssek, 2014).



516

517

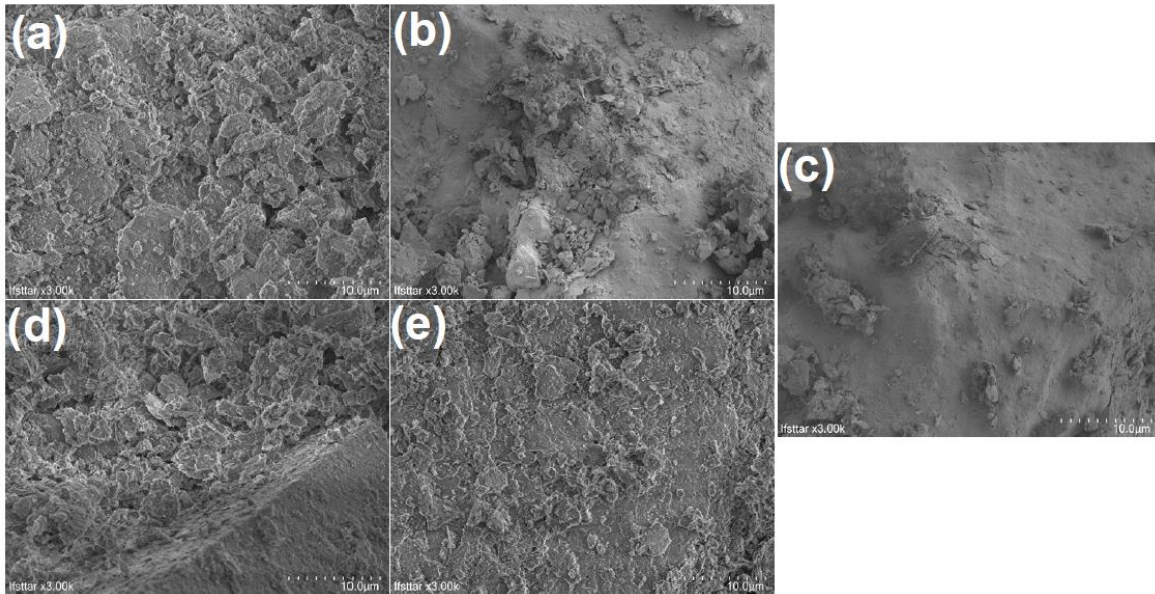
Fig. 9- SEM images for the Earth material (a) and RA-S (b).

518

519 Fig. 10 shows the SEM microstructure for the bricks fired at 800°C. The sample made
 520 with 100% of earth material revealed flower-like grains that are partially connected, and
 521 some cavities are observed, which can infer the presence of some porosity. The brick made
 522 with 100% of RA-S presented different microstructure in comparison to 100%earth material
 523 (see Fig. 9a and b). It showed a smooth surface with no apparent porosity, probably due to
 524 the crystallization and vitrification of some elements such as calcium, carbonate and other
 525 compounds derived from cement, as mentioned in the XRF and XRD analyses.

526 The brick made with 70% of earth material and 30% of RA-S (Fig. 10c) showed
 527 similar morphology in comparison with the brick prepared with 100% earth material. This
 528 highlights that an increasing in the content of earth material in the brick might harm the brick
 529 structure. This statement is corroborated by Fig. 10d and e, which have less earth material
 530 content and presented surfaces with no cavities and therefore, less porosity.

531 The brick prepared with 70% RA-S showed homogenous and cohesive structure
 532 through microscopic observation. This was because the texture of RA-S powder is finer
 533 compared to earth material and this enables the RA-S to cover and fill gaps between the
 534 earth material and RA-S, in the mixture, yielding more cohesive, regular and connected
 535 shape (Muñoz et al., 2014; Sarani et al, 2018). This could reflect in brick with better physical
 536 properties like higher compressive strengths.



538
539
540
541

Fig. 10 - SEM images for the bricks fired at 800°C: (a) 100% Earth material, (b) 100% RA-S, (c) 70% RA-S, (d) 50% RA-S and (e) 30% RA-S.

542

3.11. Determination of thermal conductivity (TC)

543

TC refers to the heat energy, which is transferred inside of a material in the form of diffusion. TC of any brick material is measured to determine their potential application as an insulating product for building purposes. Insulator materials present a low thermal conductivity since they are manufactured to diminish the heat conduction and used to save energy (Kazmi et al.2018; Sutcu et al., 2014).

548

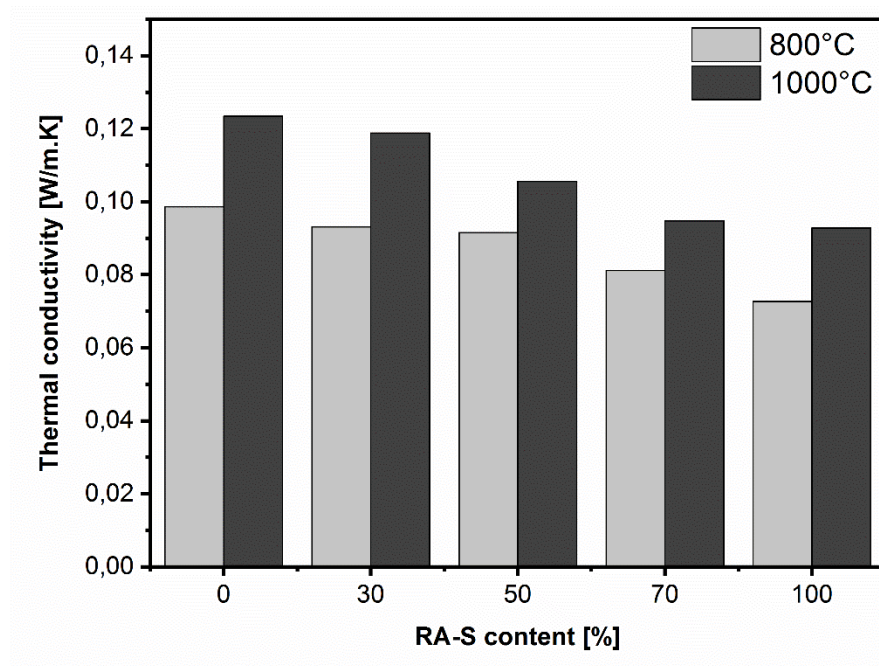
The thermal conductivity of the bricks varied accordingly to the RA-S content. In general, the thermal conductivity of the fired bricks decreased with the addition of RA-S (see Fig. 11). This trend was observed for the bricks fired at both temperatures 800 and 1000°C. These results make sense since the TC value of the Earth material is almost double compared with the TC value of the RA-S (see Table 2). In addition, the bricks fired at 800°C presented lower TC values compared to those fired at 1000°C.

554

The thermal conductivity values of the fired bricks might be linked to the brick densities (Kazmi et al.2018). In general, the density of fired bricks is considered an important characteristic that influences their thermal performances (Kazmi et al.2018; Sutcu et al., 2014). Comparing the TC with the density data, it is possible to see that the brick made with 100% of RA-S presented the lowest TC value, which also presented the lowest bulk density value (see Fig. 6). Then, a trend is observed, bricks with higher densities obtained higher TC values (see Fig. 6 and 11). This trend was also observed by Kazmi et al. (2018) that showed positive relation among density and TC of brick specimens made by adding waste glass sludge.

562

563 Therefore, it is possible to infer that the RA-S presented interesting insulation
564 performances and better energy efficiency in terms of energy savings.
565



566
567 **Fig. 11-** Thermal conductivity of the fired bricks according to the RA-S replacement.

568
569 *3.12. Comparison with the literature*

570 The brick quality depends on many factors such as raw material characteristics,
571 preparation brick process (molding), drying procedure and firing process (Al-Fakih et al.,
572 2019; Murmu and Patel, 2018). These factors will affect the quality/properties of the final
573 product, such as density, compressive strength, thermal properties, etc. Numerous
574 researchers have been studied the effect of different waste materials as an additive for fired
575 brick manufacturing. **Table 6** summarizes the results of many studies found in literature
576 concerning the use of different wastes to prepare fired bricks.

577 As previously discussed, good quality bricks also have high compressive strength. By
578 **Table 6** is possible to observe that the use of different wastes should result in bricks with
579 different properties, which can also be affected by different preparation methods.

580 Adazabra et al. (2017a) evaluated the addition of spent shea waste (SSW) for
581 manufacturing fired bricks (see **Table 6**). The increasing addition of SSW provoked an
582 increase in water absorption and a decrease in the CS, and the bricks were categorized as
583 non-load-bearing structural construction.

584 Comparing the results of this work to the results showed in **Table 6**, it is worthwhile to
585 say that RA-S is a promising material for brick production since it presents higher
586 compressive strengths when compared to several works highlighted in **Table 6**. Besides, the

587 bricks made with RA-S exhibited better insulation properties when compared with pure Earth
 588 material.

589

590 Table 6 - Summary of findings from the literature of bricks made by various wastes.

| Type of Waste | Replacement rate (%) | Experimental conditions | Main Physical characteristics | Ref. |
|-------------------------------|-------------------------|--|---|------------------------------------|
| Construction debris | 10, 20, 30 and 40 | air-dry over three days Fired at 900 and 1000°C Holding time = 4h | Compressive strength = 4.61 MPa; Water absorption (WA) = 10.28% | Sumathi (2016) |
| Agricultural wastes | 5, 10 and 20 | Fired at 900 and 1000°C Holding time = 1h | Compressive strength = 3.3 - 9.5 MPa Density = 1300–1800 kg/m ³ Open porosity = 34 – 49% | Kizinievič et al. (2018) |
| waste glass sludge | 5, 10, 15, 20 and 25 | sun-dried for 2 days and then burnt for 36 h inside the kiln at approximately 850°C Unit size = 228x114x76 mm | Compressive strength = 12.56 MPa Density = 1350–1370 kg/m ³ thermal conductivity = 0.4 - 0.7 W/mK | Kazmi et al. (2018) |
| Tannery sludge | 10 - 40 | Hand holding, then 24 h natural drying, 48 h of oven drying (105°C) and heated at 900, 950, and 1000°C Unit size = 20×60×35mm | CS: ranged from 10.98 to 29.61 MPa WA: increased from 7.2% to 20.9% | Juel et al., 2017 |
| Waste from coal beneficiation | 5, 10, 20 and 30 | Fired at 1050–1070°C | Compressive strength = 8.1 Mpa Water absorption = 15% | (Boltakova et al. (2017) |
| spent shea waste | 5, 10, 15 and 20 | mold compressed then fired at 900 or 1200°C for 1 h | Compressive strength up to 14.3 Mpa | Adazabra et al., 2017 |
| Rice husk ash | 0, 2, 4, 8, 6, 10 | Molded and fired in an industrial scale Kiln (600–850°C) Unit size = 95×95×50mm | CS ranged from 3.7 to 1.9 MPa Bulk density ranged from 1450 to 1220 kg/m ³ Thermal properties improved | De Silva and Pereira 2018 |
| Waste coal | 0, 5, 10, 15, 20 and 30 | Air drying, fired at 1000°C Unit size = 50×120×65mm | Bulk density ranged from 1040 to 1250 kg/m ³ CS ranged from 11.8 to 13.2 MPa Porosity increased | Abdrakhimov and Abdrakhimova, 2017 |
| Arsenic-iron sludge | 3, 6, 9 and 12 | Oven drying at 105°C for 2 d, fired at 1000°C in a kiln for 12 h Unit size = 250×125×75mm | CS ranged from 15.1 to 7.1 MPa WA increased from 15% | Hassan et al., 2014 |
| Diatomaceous earth residues | 3, 4, 6, 8 and 10 | Molded and burnt under 850, 950 and 1050°C Unit size = 20×28×18mm | Compressive strength ranged from 12.7 to 9.5 MPa Porosity increased by 37 vol% Thermal conductivity decreased | Galán-Arboledas et al., 2017 |
| RA-S | 0, 30, 50, 70 and 100 | dried over 1 day at 45°C followed by oven drying at 105°C for 1 day burnt under 800 and 1000°C Holding time = 2h | Compressive strength of 16.3 MPa with 70% of RA-S and fired at 800°C | This work |

591

592 **4. Conclusions**

593 In this investigation, sludge from the inert mineral part of the construction and
594 demolition waste (RA-S) obtained from the recycling aggregates plant was used as raw
595 material to prepare fired brick. The main conclusions are the following.

- 596 • The fraction of RA-S with a particle size below 2.0 mm, which is used in this
597 research work and generally rejected in most of the recycling plants, was
598 confirmed as possible substitute of natural clay for fired brick preparation
599 which can meet the requirements of many Standards all over the World.
- 600 • XRD results indicated that the bricks fired at 800°C presented different
601 microstructures when compared with bricks fired at 1000°C which reflected in
602 their physical characteristics. The SEM images indicated a more cohesive
603 microstructure for the bricks made with higher RA-S contents.
- 604 • The compressive strength of the fired bricks was influenced by both firing
605 temperature and RA-S content. The bricks fired at 800°C presented the
606 highest compressive strengths when compared with bricks fired at 1000°C.
607 The addition of up to 70% of RA-S produced the bricks with the highest
608 compressive strengths at both temperatures (800 and 1000°C).
- 609 • The densities of the bricks were not significantly affected by the firing
610 temperature. However, the bricks fired at 800°C exhibit slightly higher bulk
611 density than those fired at 1000°C. In addition the RA-S content slightly
612 decreased the densities of the fired bricks.
- 613 • The thermal conductivity results prove that RA-S has better insulation
614 properties when compared with earth material.

615 Taking into account the results obtained in this investigation, the authors recommend
616 the addition of up to 70% of RA-S to fabricate fired bricks, as this produced good quality
617 bricks in terms of their physical and mechanical properties. Therefore, the use of RA-S could
618 have practical applications in terms of recycling aspects by providing energy savings and
619 helping to boost the sustainable development and circular economy during the manufacturing
620 process of construction materials.

621

622 **Acknowledgment**

623 The authors are also grateful to the Council for the Development of Higher Education at
624 Graduate Level, Brazil (CAPES) for the postdoctoral scholarship granted through the
625 National Postdoctoral Program (PNPD).The authors also thank Mr. Ferro, president of
626 Esterel Terrassement for financial support and for providing the RA-S samples.Dr. Simoes
627 dos Reis gives a special thanks to the cooperation opportunity between UFRGS and
628 IFSTTAR through his Post-doctoral studies provided by PNPd.E.C. Lima thanks to

629 Foundation for Research Support of the State of Rio Grande do Sul (FAPERGS), and
630 National Council for Scientific and Technological Development (CNPq, Brazil) for financial
631 support and sponsorship.

632

633 **References**

634 Abdrakhimov, V.Z., Abdrakhimova, E.S., 2017. Promising use of waste coal in the production
635 of insulating material without the use of traditional natural materials, *Inorg. Mater.*
636 *Appl. Res.* 8 (5), 788–794.

637 Adazabra, A.N., Viruthagiri, G., Kannan, P., 2017a. Influence of spent shea waste addition
638 on the technological properties of fired clay bricks, *J. Build. Eng.* 11, 166–177

639 Adazabra, A.N., Viruthagiri, G., Shanmugam, N., 2017b. Infrared analysis of clay bricks
640 incorporated with spent shea waste from the shea butter industry, *J. Environ. Manag.*
641 191, 66–74.

642 AFNOR, 1993. NF P 94-051; Soils: Investigation and Testing e Determination of Atterberg's
643 Limits e Liquid Limit Test Using Casagrande Apparatus e Plastic Limit Test on Rolled
644 Thread

645 Agarwal, S., 2006. Actividad puzolánica de diversos materiales silíceos, *Cem. Concr. Res.*
646 36, 1735–1739.

647 Al-Fakih, A., Mohammed, B.S., Liew, M.S., Nikbakht, E., 2019. Incorporation of waste
648 materials in the manufacture of masonry bricks: An updated review, *J. Build. Eng.* 21,
649 37–54

650 Behera, M., Bhattacharyya, S., Minocha, A., Deoliya, R., Maiti, S., 2014. Recycled aggregate
651 from C&D waste & its use in concrete—a breakthrough towards sustainability in the
652 construction sector: A review. *Constr. Build. Mater.* 68, 501–516.

653 Bruno, A. W., Gallipoli, D., Perlot, C., Mendes, J. (2019). Optimization of bricks production by
654 earth hypercompaction prior to firing. *J. Cleaner Prod.* 214, 475-482.

655 Chen, Y., Zhang, Y., Chen, T., Liu, T., Huang, J., 2013. Preparation and characterization of
656 red porcelain tiles with hematite tailings, *Constr. Build. Mater.* 38, 1083–1088.

657 Chidiac, S.E., Federico, L.M., 2007. Effects of waste glass additions on the properties and
658 durability of fired clay brick. *Can. J. Civ. Eng.* 34, 1458-1466.

659 De Silva, G.H.M.J.S., Perera, B.V.A., 2018. Effect of waste rice husk ash (RHA) on
660 structural, thermal, and acoustic properties of fired clay bricks, *J. Build. Eng.* 18, 252–
661 259.

662 Dean, W. E. Jr., 1974. Determination of carbonate and organic matter in calcareous
663 sediments and sedimentary rocks by loss on ignition: Comparison with other
664 methods. *J. Sed. Petrol.* 44: 242–248.

665 Demir, I., 2008. Effect of organic residues addition on the technological properties of clay
666 bricks, *Waste manage.* 28, 622-627.

667 Dhanapandian, S., Gnanavel, B., 2009. Using Granite and Marble Sawing Power Wastes in
668 the Production of Bricks: Spectroscopic and Mechanical Analysis, *Research Journal*
669 *of Applied Sciences, Eng. Technol.* 2(1), 73-86.

670 Dizhur, D., Lumantarna, R., Biggs, D.T., Ingham, J.M., 2016. In-situ assessment of the
671 physical and mechanical properties of vintage solid clay bricks, *Mater. Struct.* 50 (1),
672 1–14.

673 Djomgoue, P., Njopwouo, D., 2013. FT-IR Spectroscopy Applied for Surface Clays
674 Characterization, *J. Surf. Eng. Mat. Adv. Technol.* 3, 275-282

675 Eliche-Quesada, D., Sandalio-Pérez, J.A., Martínez-Martínez, S., Pérez-Villarejo, L.,
676 Sánchez-Soto, P.J., 2018. Investigation of the use of coal fly ash in eco-friendly
677 construction materials: fired clay bricks and silica-calcareous non fired bricks,
678 *Ceramics Inter.* 44, 4400–4412

679 Galán-Arboledas, R.J., Cotes-Palomino, M.T., Bueno, S., Martínez-García, C., 2017.
680 Evaluation of spent diatomite incorporation in clay-based materials for lightweight
681 bricks processing, *Constr. Build. Mater.* 144, 327–337.

682 Goel, G., Kalamdhad, A.S., 2017. Degraded municipal solid waste as a partial substitute for
683 manufacturing fired bricks, *Const. Build. Mat.* 155, 259–266

684 Grossmann, L., Tomas, J., Csöke, B., 2004. Compressibility and flow properties of a
685 cohesive limestone powder in a medium pressure range. *Granul. Matter* 6, 103–109

686 Hassan, K.M., Fukushi, K., Turikuzzaman, K., Moniruzzaman, S.M., 2014. Effects of using
687 arsenic-iron sludge wastes in brick making, *Waste Manag.* 34 (6), 1072–1078.

688 Hir, L. P., Cayocca, F., Waeles, B., 2011. Dynamics of sand and mud mixtures: A multi
689 process-based modelling strategy, *Cont. Shelf Res.* 31, S135–S149

690 Jianu, N.R., Moga, I.C., Pricop, F., Chivoiu, A., 2018. Wastewater Sludge Used as Material
691 for Bricks Fabrication, *IOP Conference Series: Mat. Sci. Eng.* 374, 012061

692 Juel, M.A.I., Mizan, A., Ahmed, T., 2017. Sustainable use of tannery sludge in brick
693 manufacturing in Bangladesh, *Waste Manag.* 60, 259–269.

694 Karaman, S., Ersahin, S., Gunal, H. (2006). Firing temperature and firing time influence on
695 mechanical and physical properties of clay bricks. *J. Sci. Indus. Res.* 65(2), 153-159.

696 Kazmi, S.M.S., Abbas, S., Nehdi, M.L., Saleem, M.A., Munir, M.J., 2017a. Feasibility of using
697 waste glass sludge in the production of eco-friendly clay bricks. *J. Mater. Civ. Eng.*
698 29(8) 04017056

699 Kazmi, S.M.S., Munir, M.J., Abbas, S., Saleem, M.A., Khitab, A., Rizwan, M., 2017b.
700 Development of lighter and eco-friendly burnt clay bricks incorporating sugarcane
701 bagasse ash. *Pak. J. Eng. Appl. Sci.* 21, 1-5.

702 Kazmi, S.M.S., Munir, M.J., Wu, Y-F., Hanif, A., Patnaikuni, I., 2018. Thermal performance
703 evaluation of eco-friendly bricks incorporating waste glass sludge, *J. Cleaner Prod.*
704 172, 1867-1880

705 Leonel, R.F., Folgueras, M.V., Dalla Valentina, L.V.O., Prim, S.R., Prates, G.A., Caraschi,
706 J.C., 2017. Characterization of soil-cement bricks with the incorporation of used
707 foundry sand, *Cerâmica* 63, 329-335

708 Li, J., Lv, Y., Jiao, X., Sun, P., Li, J., Wuri, L., Zhang, T.C., 2020. Electrolytic manganese
709 residue based autoclaved bricks with Ca(OH)₂ and thermal-mechanical activated K-
710 feldspar additions, *Const. Build. Mat.* 230, 116848

711 Luo, L., Li, K., Fu, W., Liu, C., Yang, S., 2020. Preparation, characteristics and mechanisms
712 of the composite sintered bricks produced from shale, sewage sludge, coal gangue
713 powder and iron ore tailings, *Const. Build. Mat.* 232, 117250

714 Mbumbia, L., de Wilmar, A. M. (2002). Behaviour of low-temperature fired laterite bricks
715 under uniaxial compressive loading. *Constr. Build. Mater.* 16(2), 101-112.

716 Mo, L., Zhang, F., Deng, M., Jin, F., Al-Tabbaa, A., Wang, A., 2017. Accelerated carbonation
717 and performance of concrete made with steel slag as binding materials and
718 aggregates. *Cem. Concr. Compos.* 83, 138–145.

719 Monteiro, S.N., Vieira, C.M.F., 2014. On the production of fired clay bricks from waste
720 materials: A critical update. *Construction and Building Materials* 68, 599–610.

721 Moreno-Pérez, E., Hernández-Ávila, J., Rangel-Martínez, Y., Cerecedo-Sáenz, E., Arenas-
722 Flores, A., Reyes-Valderramiha, M.I., Salinas-Rodríguez, E., 2018. Chemical and
723 Mineralogical Characterization of Recycled Aggregates from Construction and
724 Demolition Waste from Mexico City, *Minerals* 8, 237, 2-12

725 Mubiayi, M.P., Makhatha, M.E, Akinlabi, E.T., 2018. Characterization, leachate
726 Characteristics and compressive strength of Jarosite/clay/fly ash bricks, *Materials*
727 *Today: Proceedings* 5 (2018) 17802–17811

728 Murmu, A.L. Patel, A., 2018. Towards sustainable bricks production: An overview,
729 *Construction and Building Materials* 165, 112–125

730 Murray, H.H., 1991. Overview: clay mineral applications, *Appl. Clay Sci.* 5 (5–6), 379–395.

731 Musthafa, A.M., Janaki, K., Velraj, G., 2010. Microscopy, porosimetry and chemical analysis
732 to estimate the firing temperature of some archaeological pottery shreds from India,
733 *Microchem. J.* 95, 311–314.

734 Poon, C.S., Kou, S.C., Lam, L., 2002. Use of recycled aggregates in molded concrete bricks
735 and blocks, *Constr. Build. Mater.* 16, 281–289.

736 Poon, C.S., Kou, S.C., Wan, H., Etxeberria, M., 2009. Properties of concrete blocks prepared
737 with low grade recycled aggregates. *Waste Manag.* 29, 2369–2377.

738 Poullain, P., Mounanga, P., Bastian, G., and Coué, R. 2006. Determination of the
739 thermophysical properties of evolutive porous materials. *Eur. Phys. J. Appl. Phys.* 33,
740 35-49

741 Raut, S.P., Ralegaonkar, R.V., Mandavgane, S.A., 2011. Development of sustainable
742 construction material using industrial and agricultural solid waste: A review of waste-
743 create bricks. *Construction and building materials* 25, 4037–4042.

744 Riaz, M.H., Khitab, A., Ahmed, S., 2019. Evaluation of sustainable clay bricks incorporating
745 Brick Kiln Dust. *Journal of Building Engineering* 24, 100725.

746 Rukijkanpanich, J., Thongchai, N., 2019. Burned brick production from residues of quarrying
747 process in Thailand, *J. Building Eng.* 25:100811

748 Russ, W., Mortel, H., Meyer-Pittroff, R., Babeck, A., 2006. Kieselguhr sludge from the deep
749 bed filtration of beverages as a source for silicon in the production of calcium silicate
750 bricks, *J. Eur. Ceram. Soc.* 26, 2547–2559.

751 Saleem, M.A., Kazmi, S.M.S., Abbas, S., 2017. Clay bricks prepared with sugarcane
752 bagasse and rice husk ash – A sustainable solution, *MATEC Web of Conferences*
753 120, 03001

754 Santisteban, J.I., Mediavilla, R., Lopez-Pamo, E., Dabrio, C.J., Zapata, M.B.R., Garcia,
755 M.J.G., Castano, C., Alfaro, P.E.M., 2004. Loss on ignition: a qualitative or
756 quantitative method for organic matter and carbonate mineral content in sediments?,
757 *Journal of Paleolimnology* 32: 287–299

758 Sarani, N.A., Kadir, A.A., Rahim, A. S.A., Mohajerani, A., 2018. Properties and
759 environmental impact of the mosaic sludge incorporated into fired clay bricks,
760 *Construction Build. Mater.* 183, 300–310

761 Sutcu, S.M., Akkurt, S., 2009. The use of recycled paper processing residues in making
762 porous brick with reduced thermal conductivity, *Ceramics Inter.* 35, 2625–2631

763 Ukwatta, A., Mohajerani, A., 2017. Characterisation of fired-clay bricks incorporating
764 biosolids and the effect of heating rate on properties of bricks, *Const. Build. Mat.* 142,
765 11–22

766 Velasco, P.M., Ortíz, M.P., Giró, M.A.M., Velasco, L.M., 2014. Fired clay bricks manufactured
767 by adding wastes as sustainable construction material – A review, *Constr. Build.*
768 *Mater.* 63, 97–107.

769 Vieira, C.M.F., Monteiro, S. N., 2006. Effect of the Particle Size of the Grog on the Properties
770 and Microstructure of Bricks, *Mat. Sci. Forum*, 530-531, 438-443.

771 Viruthagiri, G., Priya, S.S., Shanmugam, N., Balaji, A. Balamurugan, K. Gopinathan, E.,
772 2015. Spectroscopic investigation on the production of clay bricks with SCBA waste,
773 *Spectrochim. Acta, Part A* 149, 468–475.

- 774 Yoo, J., Shin, H., Ji, S., 2018. Evaluation of the Applicability of Concrete Sludge for the
775 Removal of Cu, Pb, and Zn from Contaminated Aqueous Solutions, *Metals* 8, 666
- 776 Zhang, J., Shi, C., Li, Y., Pan, X., Poon, C-H., Xie, Z., 2015. Performance Enhancement of
777 Recycled Concrete Aggregates through Carbonation, *J. Mater. Civ. Eng.* 27(11):
778 04015029
- 779 Zhang, P., Huang, J., Shen, Z., Wang, X., Luo, F., Zhang, P., Wang, J., Miao, S., 2017. Fired
780 hollow clay bricks manufactured from black cotton soils and natural pozzolans in
781 Kenya, *Constr. Build. Mater.* 141, 435–441